J. Fluid Mech. (1998), *vol.* 362, *pp.* 199–227. Printed in the United Kingdom

Laminar free convection induced by a line heat source, and heat transfer from wires at small Grashof numbers

By AMABLE LIÑÁN AND VADIM N. KURDYUMOV

E.T.S. Ingenieros Aerouticos, Plaza Cardenal Cisneros 3, Universidad Politécnica de Madrid, 28040 Madrid, Spain

(Received 6 March 1997 and in revised form 17 December 1997)

The buoyancy-induced laminar flow and temperature fields associated with a line source of heat in an unbounded environment are described by numerically solving the non-dimensional Boussinesq equations with the appropriate boundary conditions. The solution is given for values of the Prandtl number, the single parameter, ranging from zero to infinity. The far-field form of the solution is well known, including a self-similar thermal plume above the source. The analytical description close to the source involves constants that must be evaluated with the numerical solution.

These constants are used when calculating the free convection heat transfer from wires (or cylinders of non-circular shape) at small Grashof numbers. We find two regions in the flow field: an inner region, scaled with the radius of the wire, where the effects of convection can be neglected in first approximation, and an outer region where, also in first approximation, the flow and temperature fields are those due to a line source of heat. The cases of large and small Prandtl numbers are considered separately. There is good agreement between the Nusselt numbers given by the asymptotic analysis and by the numerical analysis, which we carry out for a wide range of Grashof numbers, extending to very small values the range of existing numerical results; there is also agreement with the existing correlations of the experimental results. A correlation expression is proposed for the relation between the Nusselt and Grashof numbers, based on the asymptotic forms of the relation for small and large Grashof numbers.

1. Introduction

The study of natural convection induced by heated horizontal circular cylinders in an infinite fluid space has received much attention in the literature, due to the role it plays in many engineering and scientific problems. See Gebhart *et al.* (1988) for an extensive review of these studies. Most of them correspond to cases with large Grashof numbers, when heat conduction and viscous forces are confined to thin free convection boundary layers followed by thin thermal plumes above the cylinders. A number of studies, beginning with the work of Hermann (1936), have been devoted to the description of these boundary layers and plumes, based on the boundary layer approximation of the Boussinesq equations. Numerical investigations, also based on the Boussinesq equations, have been carried out, for large and moderate Rayleigh numbers, by, among others, Kuehn & Goldstein (1980), Farouk & Güçeri (1981) and Saitoh, Sajik & Maruhara (1993). Solutions have been given in the literature for a

wide range of Rayleigh numbers, $10^0 \leqslant Ra \leqslant 10^7$, but not for the cases of small and extremely small Rayleigh numbers to be considered in this paper.

The plumes generated by free convection above heated cylinders have also been widely investigated, beginning with the pioneering work of Zeldovich (1937). He was the first to understand that the flow takes an asymptotic self-similar form far above the cylinder. The far-field distributions of temperature and velocity are determined by the heat lost by the cylinder, independently of its size and shape, as a line source of heat. The equations describing the self-similar flow structure were written later by Schuh (1948), Yih (1952, 1969), and independently by Mahony (1957). Yih solved the equations in closed form for two values of the Prandtl number, $Pr = 5/9$ and 2. Numerical solutions of the self-similar equations were given later by Fujii (1963), Gebhart, Pera & Schorr (1970) and Fujii, Morioka & Uehara (1973). The first term in an asymptotic description for $Pr \gg 1$ was obtained by Spalding & Cruddace (1961) and by Kuiken & Rotem (1971), who also analysed the case $Pr \ll 1$. It is remarkable that the analogous asymptotic structure, for $Pr \gg 1$, of the plume above a point source of heat has been given only recently by Vázquez, Pérez & Castellanos (1996).

With the aim of resolving discrepancies between the self-similar predictions and experiments, higher-order effects, in an expansion for large distances above the line source, have been studied by Riley (1974) and by Hieber & Nash (1975), who also looked at the stability of the plume, previously analysed by Haaland & Sparrow (1974). Higher-order effects for the far-field behaviour of free convection plumes from line sources on a wall have been considered by Mörwald, Mitsotakis & Schneider (1986). The structure and stability of the buoyant plumes above heated wires and line sources of heat in a bounded region has also been numerically analysed by Desrayaud & Lauriat (1993), Deschamps & Desrayaud (1994) and Lauriat & Desrayaud (1994) using the Boussinesq equations. Their analysis of free convection from heated wires was mainly concerned with the description of the instabilities that lead to a meandering motion of the plume far above the source, which is independent of the details of the flow near the heat source. They did not cover the low Grashof number cases, and their line source calculations use a mesh too coarse near the source to give a description accurate enough for the evaluation of the flow around thin wires and the Nusselt number dependence on the Grashof number.

A first attempt to analyse the flow structure at low Grashof numbers appears in Mahony (1957). Understanding that in this case the temperature distribution close the wire is dominated by heat conduction, he obtained an approximate theoretical correlation of the Nusselt and Grashof numbers, by joining smoothly, at a point on the symmetry plane above the cylinder, the temperature of the solution of the heat conduction equation around the cylinder and the centreplane temperature of the similarity solution for the plume. Although the two distributions do not match, this correlation was found to compare well with the experimental results of Collis & Williams (1954). Nakai & Okazaki (1975) used a patching procedure, similar to that of Mahony, and obtained a correlation formula by equating the circumferential average temperature given by heat conduction in a concentric surface around the cylinder to that in the plume above the cylinder. A numerical analysis based on an approximate form of the equations, valid only for $Gr \gg 1$, was used by Fujii, Fujii & Matsunaga (1979) to calculate the Nusselt number and to propose a correlation of the experimental results, aiming to cover the range $10^{-10} < Ra < 10^7$. An approximate analysis of the free convection heat transfer from thin wires in porous media has been given by Ingham & Pop (1987), using also the approach of Mahony.

In this paper we deal with the pure free convection flow and heat transfer from horizontal, infinitely long, circular cylinders. We shall be concerned, mainly, with the cases, which have received less attention in the literature, in which the size l_h of the heated region surrounding the wire is not small compared with its radius a. For example, for gases, with $Pr \sim 1$, these cases correspond to Grashof numbers of order unity, when $l_h \sim a$, or small compared with 1, when $l_h \gg a$. They are encountered at low pressures or at microgravity conditions.

The analysis will be based on the numerical solution of the Boussinesq equations, written in non-dimensional form in § 2 after identifying the scales encountered in the analysis of the cases $Gr \lesssim 1$. For $Gr \ll 1$ the flow structure is well represented by that of a line source of heat, described in § 3 for $Pr \sim 1$, in § 4 for $Pr \gg 1$, and in Appendix A for $Pr \ll 1$. Section 5 is devoted to the description of the results of the numerical analysis of the cases $Gr \sim 1$ and to the asymptotic analysis of the cases with $Gr \ll 1$. Section 6 will be devoted to the conclusions and generalization of the results of our asymptotic analysis for $a/l_h \to 0$ to deal with non-circular cylinder shapes and non-Boussinesq effects.

2. Formulation

The free convection problem will be posed in this paper as to find the surface temperature, T_w, of the wire that results in a given heat loss rate, q, per unit length. We proceed in this way because, as shown by Zeldovich (1937), q determines the far-field distributions of velocity and temperature that we need to describe to obtain the numerical solution. We shall be concerned with the free convection flow induced by heated horizontal or inclined, infinitely long, wires. For an infinitely long wire the temperature distribution and, therefore, the heat transfer from the wire are not affected by the gravity component g_l in the direction of the wire. The temperature distribution and the flow field transverse to the wire axis are two-dimensional, determined by the corresponding gravity component g_n. The velocity field parallel to the wire axis, induced by the longitudinal buoyancy force proportional to the gravity component g_l, is given by a linear equation, whose numerical solution for a line source of heat is described in Appendix B.

In our analysis we shall use the Boussinesq approximate form of the conservation equations, based on the assumption that the density variations, when measured with the far-field density, are small compared with unity. They are given by the product, $-\beta(T - T_\infty)$, of the volumetric thermal expansion coefficient β and the temperature variations, and when multiplied by the acceleration due to gravity $\boldsymbol{g}$ determine the buoyancy force per unit mass. For gases the Boussinesq approximations are conditioned to the requirement $T - T_\infty \ll T_\infty$; then, $\beta = 1/T_\infty$ and the kinematic viscosity, ν, and the thermal diffusivity, α, can be considered as constant.

The only parameters appearing in the Boussinesq equations are $g\beta$, ν and α, while two additional parameters enter in the boundary conditions: the ratio q/λ_∞ of the heat source strength and heat conductivity, and the wire radius a (or an equivalent length scale for cylinders of non-circular shape).

It is important to observe that $g\beta$, α and q/λ_∞ define the scales

$$l_h = (g\beta q/\lambda_\infty \alpha^2)^{-1/3}, \quad v_h = (\alpha g\beta q/\lambda_\infty)^{1/3}, \quad (T_h - T_\infty) = q/\lambda_\infty \tag{2.1}$$

which can be used to measure the spatial coordinates $\boldsymbol{x}'$, velocity $\boldsymbol{v}'$ and temperature variations $T - T_\infty$, when writing the Boussinesq equations and boundary conditions

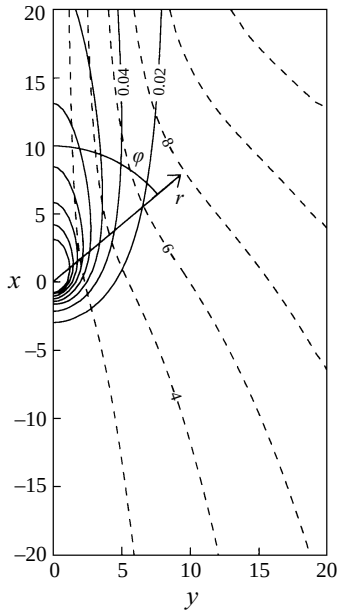

FIGURE 1. The system of coordinates, the streamlines (dashed lines) and isotherms (solid lines) around the line source of heat, computed for $Pr = 0.72$. Gravity acts in the negative x-direction.

in non-dimensional form. These equations, using the cylindrical coordinates $r = r'/l_h$ and the angle φ with the vertical direction, defined in figure 1, take the form

$$\omega = -\Delta\psi, \tag{2.2}$$

$$v_r \frac{\partial \omega}{\partial r} + \frac{v_\varphi}{r}\frac{\partial \omega}{\partial \varphi} = Pr\Delta\omega - \left(\sin\varphi \frac{\partial \theta}{\partial r} + \frac{\cos\varphi}{r}\frac{\partial \theta}{\partial \varphi}\right), \tag{2.3}$$

$$\left(v_r \frac{\partial \theta}{\partial r} + \frac{v_\varphi}{r}\frac{\partial \theta}{\partial \varphi}\right) = \Delta\theta, \tag{2.4}$$

in terms of the non-dimensional temperature rise $\theta = (T - T_\infty)/(T_h - T_\infty)$, stream function ψ, and vorticity ω. The velocity components, $v_r = r^{-1}\psi_\varphi$, $v_\varphi = -\psi_r$, and θ, ω and ψ are 2π-periodic functions of φ; θ is symmetric and ω and ψ antisymmetric in φ.

For the boundary conditions, we require

$$\theta \to 0, \qquad \boldsymbol{v} \to 0 \qquad \text{at} \qquad r \to \infty \tag{2.5}$$

outside a slender thermal plume above the source, where, as shown in § 3.3, $r \gg 1$ and $\varphi \sim r^{-3/5}$, $v_r \sim r^{1/5}$. The conditions at the wire surface, representing non-slip of the velocity and the given heat output from the wire, take the form

$$r = a/l_h = \varepsilon : \qquad \int_0^{2\pi} r\frac{\partial \theta}{\partial r}\mathrm{d}\varphi = -1, \quad \theta = \theta_w, \qquad \boldsymbol{v} = 0, \tag{2.6}$$

where the value θ_w of the wire surface temperature, assumed to be uniform, is to be calculated.

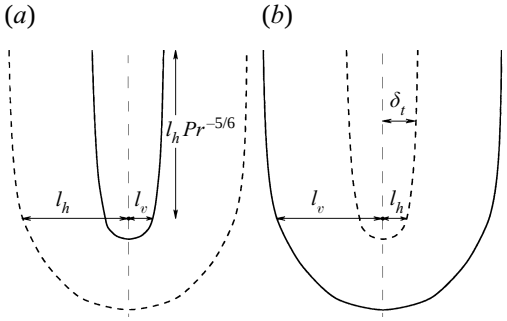

FIGURE 2. Sketch of the shape and position of the thermal (solid lines) and viscous (dashed lines) regions for (*a*) $Pr \ll 1$ and (*b*) $Pr \gg 1$. In both cases $l_v = Prl_h$.

The only parameters left in the formulation are the Prandtl number, $Pr = \nu/\alpha$, and the non-dimensional radius of the wire

$$\varepsilon = a/l_h = (a^3 g\beta q/\lambda_\infty \alpha^2)^{1/3}. \tag{2.7}$$

Notice that $\varepsilon^3 Pr^{-2}$ is the Grashof number based on a and the temperature difference q/λ_∞.

The solution of the problem (2.2)–(2.6) must provide the non-dimensional wire surface temperature rise $\theta_w = (T_w - T_\infty)/(T_h - T_\infty)$, or equivalently the Nusselt number

$$Nu = q/2\pi(T_w - T_\infty)\lambda_\infty = 1/2\pi\theta_w, \tag{2.8}$$

as a function of ε and Pr.

If we had posed the free convection problem in the traditional way, as to find q in terms of $(T_w - T_\infty)$, then the same equations, which include the dimensional parameters $g\beta$, ν and α, should be solved with boundary conditions where $(T_w - T_\infty)$ and a appear as additional parameters. When this problem is written in non-dimensional form, with a as length scale and $(T - T_\infty)$ measured with $(T_w - T_\infty)$, we are left with Pr and the Grashof number

$$Gr = g\beta(T_w - T_\infty)a^3/\nu^2, \tag{2.9}$$

or equivalently the Rayleigh number, $Ra = GrPr$, as the only two parameters determining the Nusselt number and the flow structure.

The relation $GrPr^2 = \varepsilon^3/2\pi Nu$ between ε and Gr is not direct, because it involves the still unknown $Nu(\varepsilon, Pr)$. However, at least for $Pr \sim 1$, when a and l_h are the only length scales in the problem, we may expect ε and Gr to grow simultaneously from small to large compared with unity. For values of Pr very small or very large compared with unity, we encounter an additional scale, l_v, the size of the region around the wire where viscous effects are important. It turns out that $l_v = l_h Pr$ (when $l_v/a \gtrsim 1$), both for small and large values of Pr, as we shall see in § 5 and in Appendix A. The structure of the solution will depend not only on $\varepsilon = a/l_h$ but also on the ratio $\hat{\varepsilon} = a/l_v = \varepsilon/Pr$. A sketch of the shape and position of the thermal and viscous regions, for line heat sources, is given in figure 2 for $Pr \gg 1$ and $Pr \ll 1$.

The cases $\varepsilon \gg 1$, corresponding to large Grashof numbers, above the line $GrPr^2$ in the (Gr, Pr)-plane of figure 3, have received much attention in the literature because they are encountered often in applications. Their analysis, as shown in Leal (1992) for example, can be carried out using the boundary layer approximation, because the heated region around the cylinder is a layer of thickness of order $a(GrPr^2)^{-1/4}$ for

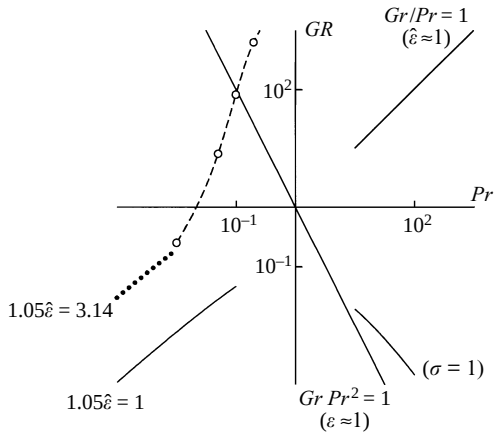

FIGURE 3. Gr, Pr parametric plane: dashed line, computed threshold values of $Gr(Pr)$ for the appearance of a recirculation bubbles; dotted line, asymptotic threshold values for $Pr \ll 1$. The flow field induced by the hot wire is that of a line source below the line $\varepsilon = 1$. Below the line $\hat{\varepsilon} = 1$, vorticity is found below the wire at distances large compared with its radius.

$Pr \leqslant 1$ and $a(GrPr)^{-1/4}$ for $Pr \gg 1$, small compared with a; the corresponding Nusselt numbers are then of order $(GrPr^2)^{1/4}$ and $(GrPr)^{1/4}$, respectively. The description in § 5 of the cases with $\varepsilon \sim 1$ is based on numerical solutions of the complete Boussinesq equations, which are used to calculate $Nu = Nu(\varepsilon, Pr)$. The numerical results show a recirculating region above the wire for values of the Grashof larger than a threshold value that depends on Pr, shown in figure 3 with a dashed line.

The cases $\varepsilon = a/l_h \ll 1$, corresponding to small Grashof numbers, can be analysed with the technique of matched asymptotic expansions, as done by Kaplun & Lagerstrom (1957) for the low-Reynolds-number flow past a cylinder. For $\varepsilon \ll 1$ and $Pr \sim 1$, we find two distinguished regions in the flow field surrounding the wire. One is an inner, Stokes-type, region scaled with a, where the temperature and velocity fields are dominated by heat conduction and viscous forces, with negligible effects of convection. The outer heated region around the wire has a much larger scale l_h, determined by the balance of conduction with the convective transport resulting from the flow induced by the buoyancy forces. The full Boussinesq equations (2.2)–(2.4) must be used to describe the flow and temperature fields in this outer region, which is the base of the self-similar free convection plume encountered at distances large compared with l_h.

When looking at the flow with the outer scale l_h, the hot cylinder appears to act, in the limit $a/l_h \to 0$, as a line source of heat. This is so in the low-Grashof-number limit, because the arresting effect of the drag of the cylinder on the free convection flow can be neglected in first approximation. For this reason, we begin with the description, in the following two Sections, of the steady laminar flow induced by a horizontal line source of heat of given strength q. In § 5 we show how this analysis can be used, with the technique of matched asymptotic expansion, to calculate the Nusselt number in free convection flows induced by heated wires at small Grashof numbers or, more precisely, for small values of ε. We use the results of the asymptotic analysis to propose a correlation of the Nusselt numbers provided by our numerical solution of the problem (2.2)–(2.6) for various finite values of ε and Pr.

3. Free convection from a line source of heat

3.1. *Formulation*

We shall describe in this Section the flow and temperature fields generated by gravity forces when a horizontal source of heat is placed in a fluid, stagnant and with a temperature T_∞ far from the source.

The analysis will be restricted to cases where the expected temperature variations $(T - T_\infty)$ are small compared with T_∞ in most of the flow field and, thus, we can use there the Boussinesq form of the conservation equations. Then, as indicated in § 2, the parameter q/λ_∞, characterizing the strength of the heat source, and the dimensional parameters $g\beta$ and α, which appear together with $\nu = \alpha Pr$ in the equations, define the characteristic values, l_h, v_h and $T_h - T_\infty$, given in (2.1), of the size of the heated region around the source, and of the velocities and temperature rise in the region.

These scales can also be obtained from three relations derived by equating the estimates of the order of magnitude of the terms of the conservation equations. Thus, from the line heat source definition we obtain $T_h - T_\infty = q/\lambda_\infty$; the balance of the convective and buoyancy terms in the momentum equation leads to $v_h^2/l_h = g\beta(T_h - T_\infty)$; and, finally, the balance in the energy equation of convection and conduction leads to $v_h l_h/\alpha = 1$. When these scales are used to formulate the problem in non-dimensional form we obtain the system (2.2)–(2.4) with the far-field conditions (2.5).

When analysing the problem of free convection from a line source the conditions (2.6) are replaced by

$$\lim_{r\to 0} \int_0^{2\pi} r \frac{\partial \theta}{\partial r} \mathrm{d}\varphi = -1, \tag{3.1}$$

corresponding to the limit $\varepsilon \to 0$ in (2.6), when $\theta_w \to \infty$ and the arresting effect of the wire disappears so that there is no source of momentum at $r = 0$. In the resulting non-dimensional formulation, appropriate for the description of the cases $Pr \lesssim 1$, the Prandtl number appears as a factor in the term representing the diffusion of vorticity.

Notice that the non-dimensional parameter $q/\lambda_\infty T_\infty$ must be small compared with unity for the Boussinesq approximations to apply in the main region, $r = r'/l_h \sim 1$, of the flow field. Even if $q/\lambda_\infty T_\infty \ll 1$, as we assume to be the case in this paper, non-Boussinesq effects associated with the variation of heat conductivity with temperature must be taken into account for $r \ll 1$, close to the line source, as we shall show in §4. Fortunately, they do not affect the description of the region $r \gtrsim 1$.

The solution of the problem (2.2)–(2.5) and (3.1), involving Pr as the single parameter, can only be obtained numerically after describing with coordinate expansions the singular form of the solution for small values of r, in § 3.2, and the well-known far-field form, for $r \gg 1$, in §3.3.

3.2. *The form of the solution in the Stokes region* $r \ll 1$

For values of $r \ll 1$, the temperature and stream function satisfy the Stokes equations, obtained from (2.2)–(2.4) by neglecting the convective terms because they involve lower derivatives. Then, for $r \ll 1$, θ, ω and ψ can be described by the expansions

$$2\pi\,\theta = -\ln r + A_0 + A_1 r \cos\varphi + \ldots, \tag{3.2}$$

$$\omega = \left\{ C_1 r - \frac{r \ln r}{4\pi Pr} \right\} \sin\varphi + \ldots, \tag{3.3}$$

$$\psi = \left\{ U_0 r + r^3 \left(\frac{\ln r - 3/4}{32\pi Pr} - \frac{C_1}{8} \right) \right\} \sin\varphi + C_2 r^2 \sin 2\varphi + \ldots, \tag{3.4}$$

where we have eliminated the solutions of the Stokes equations more singular at $r = 0$ than the solution $\ln r$, required by the heat source. The perturbations to the small-r expansion coming from the local effect of the convective terms are of order $r^2 \ln r$, or higher. They have not been included in (3.2)–(3.4) because they do not play a significant role in the numerical description for $r \ll 1$; this is also the case for the terms in (3.3) and (3.4) inversely proportional to Pr, representing the effects of the local buoyancy forces.

The constants appearing in this small-r expansion must be obtained as part of the numerical solution of the line source problem. A_0 determines the temperature level near the source, A_1 measures the vertical temperature gradient, and U_0 is the vertical velocity induced by the buoyancy forces at the line source.

3.3. *Asymptotic form of the solution for large r*

The asymptotic form of the solution of the system of equations (2.2)–(2.4) for values of $r \gg 1$, and values of $\varphi \ll 1$, is given by the well-known self-similar solution

$$\theta = r^{-3/5} G(\xi), \qquad \psi = r^{3/5} F(\xi) \tag{3.5}$$

of the boundary layer form of (2.2)–(2.4), involving the similarity variable $\xi = \varphi r^{3/5} = y/x^{2/5}$, of order unity in the thermal plume. For $r \gg 1$, outside the plume, $\theta = \omega = 0$.

The equations determining $F(\xi)$ and $G(\xi)$, first obtained by Schuh (1948) and Yih (1952), are

$$5PrF''' + 3FF'' - F'^2 + 5G = 0, \tag{3.6}$$

$$5G' + 3FG = 0, \tag{3.7}$$

to be solved, for $\xi \geqslant 0$, with the symmetry conditions $F = F'' = 0$ at $\xi = 0$, and the boundary conditions $F' = G = 0$ at $\xi \to \pm\infty$. In addition $\int_{-\infty}^{\infty} F'G\mathrm{d}\xi = 1$ must be satisfied to ensure that the vertical convective flux of energy in the plume equals the heat generated at the source.

In our analysis of the steady laminar flow, we shall use this far-field description of the plume, even though it may lose stability, as shown by Haaland & Sparrow (1973), when the Reynolds number, $\sim r^{3/5}$, based on the plume thickness is larger than a critical value, which turns out to be large compared with 1.

The numerical solution of (3.6)–(3.7) determines $F(\xi \to \infty) = F_\infty$, and thus the entrainment velocity $v_e = -(3/5)F_\infty r^{-2/5}$ by the plume. The function $F_\infty(Pr)$ has the asymptotic behaviour $F_\infty = 1.355 Pr^{2/5}$ for $Pr \to \infty$, obtained by Spalding & Cruddace (1961), and $F_\infty(0) = 1.515$, as calculated by Kuiken & Rotem (1971). The expression $F_\infty = 1.515\{1 + (1.355/1.515)^{5/2} Pr\}^{2/5}$ correlates, with errors lower than 2.5%, the numerical values that we obtained for $F_\infty(Pr)$.

As indicated before, outside the thermal plume, for large r,

$$\theta = \omega = 0, \quad \psi = F_\infty r^{3/5} \sin(3(\pi - \varphi)/5) / \sin(3\pi/5), \tag{3.8}$$

which corresponds to the irrotational flow associated with the entrainment velocity v_e, in an unbounded environment of temperature T_∞.

3.4. *Numerical solution in the main, Boussinesq, region*

From (3.2)–(3.4) it follows that the boundary conditions at $r \to 0$ for a pure line source of heat can be written in the form

$$r \to 0 : \qquad r\frac{\partial \theta}{\partial r} + \frac{1}{2\pi} = r\frac{\partial \omega}{\partial r} - \omega = r\frac{\partial \psi}{\partial r} - \psi = 0. \tag{3.9}$$

This weak form of the inner boundary conditions was imposed at $r = r_{min} \ll 1$, after writing the equations in terms of $\eta = \ln r$ in order to improve the accuracy of the numerical solution at small values of r. The numerical solution was obtained, for $0 \leqslant \varphi \leqslant \pi$, using two forms of the boundary conditions at a finite outer boundary $r = r_{max}$.

The first one was based on the self-similar solution (3.5) for the plume and on the irrotational flow (3.8) outside. We consider that ψ, ω and θ are given at the outer boundary, $r = r_{max}$, of the computational domain by the values obtained by adding the first term of the far-field asymptotic description for the plume (3.5) and for the outer region (3.8), and subtracting the common part, which is $F_\infty r^{3/5}$ for ψ.

The second form of the boundary conditions was based on the division of the boundary $r = r_{max}$ into inflow and outflow regions, with negative and positive values of the radial velocity, respectively. Using (3.8), we find that the inflow region corresponds to $\pi/6 < \varphi < \pi$, and that outflow occurs for $0 < \varphi < \pi/6$. At the inflow boundary we used (3.8), while at the outflow boundary the following mild boundary conditions were adopted:

$$\frac{\partial^2 \psi}{\partial r^2} = \frac{\partial \theta}{\partial r} = \frac{\partial \omega}{\partial r} = 0. \tag{3.10}$$

The vorticity and energy equations were solved numerically, using second-order three-point approximations for the first and second derivatives. To obtain the stationary distributions of all variables a pseudo-unsteady form of the governing equations was used. The Poisson equation was solved iteratively introducing an artificial time. To test the grid dependence, calculations were carried out using 71×71, 101×101 and 131×131 grids; the typical number was 101×101. We considered that the stationary distribution had been reached when $\max_{i,j} |f_{i,j} - \hat{f}_{i,j}| < 10^{-9}$, where f and $\hat{f}$ are the values of the temperature or the vorticity at the current and previous time levels, respectively. The typical value of the outer boundary was $r_{max} = 100$.

No significant differences were found for the velocity and temperature distributions when using the two kinds of boundary conditions, down to values of $Pr = 0.01$. For very small Pr (for example, $Pr = 0.01$), small artificial oscillations appear near the outflow boundary in the plume when the first kind of boundary condition is used; these oscillations did not appear in the calculations with the boundary conditions (3.10). No significant differences in the distributions were found in the rest of the computational domain. The calculations were carried out with different values of $\eta_{min} = \ln r_{min}$, to ensure independence from the computational domain; for values of r_{min} below 10^{-2} the changes in A_0 affect only the fourth digit.

Figures 1 and 4 show the isotherms and streamlines for different Prandtl numbers, using the scales l_h, $T_h - T_\infty$ and v_h, defined by (2.1). These figures illustrate the change in flow structure with increasing values of the Prandtl number; notice the small changes observed in the isotherms, and the increasing thickness of the viscous plume.

The vertical velocity distribution in the centreplane of the plume is shown in figure 5 for various values of Pr. Observe how the vertical velocity gradient at the line source

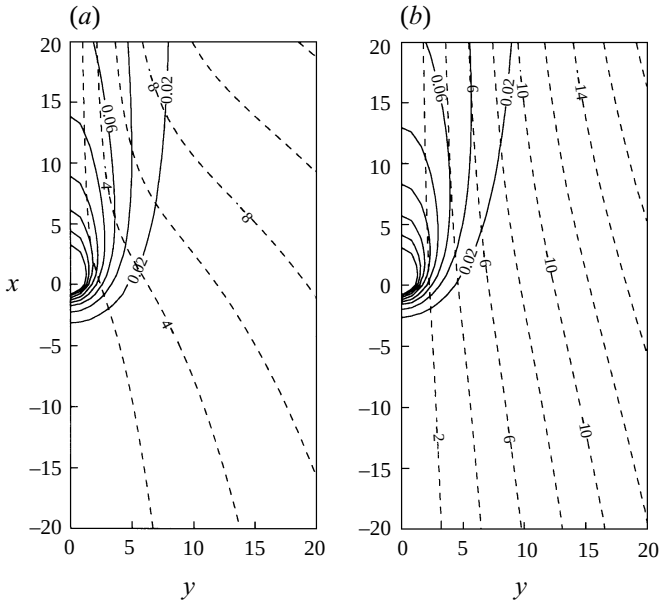

FIGURE 4. Computed streamlines (dashed lines) and isotherms (solid lines) for the line source of heat: (*a*) $Pr = 0.1$; (*b*) $Pr = 10$.

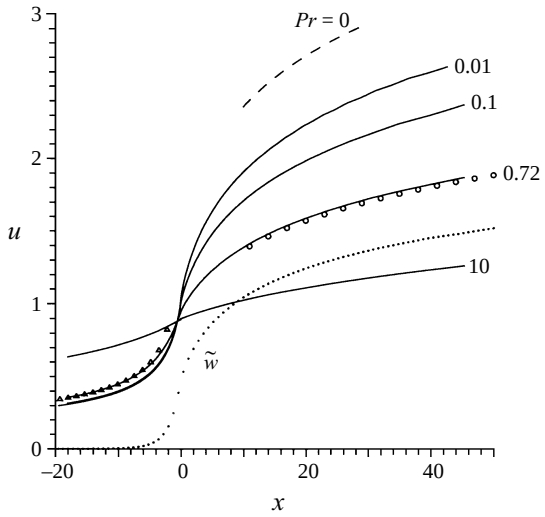

FIGURE 5. Computed vertical velocity (solid lines) in the centreplane of the plume for various Pr, and far-field asymptotic behaviour above the source for $Pr = 0.72$ (circles) and $Pr = 0$ (dashed line), and for $Pr = 0.72$ (triangles) below the source; dotted line: the centreplane longitudinal velocity $\tilde{w}$ for $Pr = 0.72$.

grows toward infinity when $Pr \to 0$. Some additional details of the flow near the pure line source at $Pr \ll 1$ are presented in Appendix A. The dashed line gives, for $Pr = 0$, the self-similar asymptotic description of the plume.

Shown in figure 6, with a solid line, is the temperature distribution along the x-axis for $Pr = 0.72$. The dashed lines correspond to the asymptotic behaviour, near the source, given by the first two terms of (3.2), and for $x \gg 1$ in the thermal plume,

Pr	0.01	0.1	0.72	1	10	∞
U_0	1.05	1.04	0.98	0.97	0.93	0.87
A_0	0.97	0.97	0.96	0.96	0.95	0.95

TABLE 1. The velocity and temperature level at the line source of heat

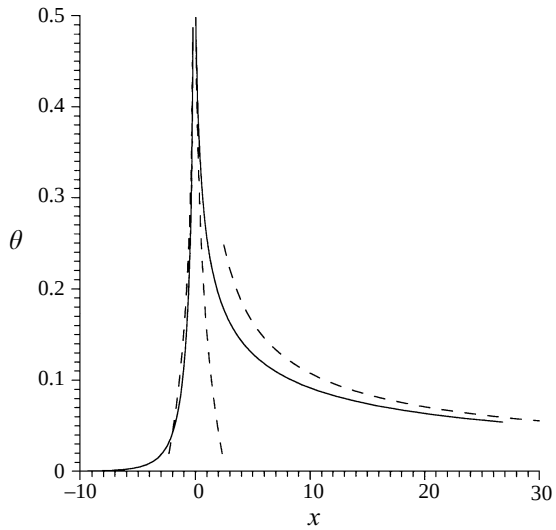

FIGURE 6. Computed temperature distribution, for $Pr = 0.72$ (solid line), at the centreplane, and its asymptotic behaviour for small and large r (dashed lines).

given by (3.5). One can see in this figure the range where the asymptotic descriptions apply.

Our primary interest lies in the numerical calculation of the constants A_0 and U_0. Table 1 shows the values of A_0 and of the velocity U_0 at the line source, for various values of the Prandtl number. We find an unexpected weak dependence on the Prandtl number of the constant A_0, which determines the temperature distribution (3.2) near the source. A_0 changes from 0.97, for small Pr, to 0.948 in the limit $Pr \to \infty$; observe also the moderately small changes of U_0 with Pr.

4. Free convection flow, due to a line source of heat, for $Pr \gg 1$

4.1. *Formulation*

At large Prandtl numbers, we encounter three distinguished regions, sketched in figure 2. A heated region surrounding the line source of size, l_h, defined by the balance of conduction and convection, with the characteristic velocity v_h – so that $v_h l_h/\alpha = 1$. This region is the base of the thermal plume, where the temperature is determined by the balance of heat conduction, transverse to the layer, and the convective transport of the heat q leaving the source. The thickness, δ_t, of this thermal layer will be found to be small compared with the size, l_v, of the viscous region surrounding the line source. In this region the motion, with a characteristic velocity v_v shared with the thermal plume and imposed on the inner heated region (so that $v_v = v_h$), is dragged by the viscous stresses that originate in the thermal plume

to balance the buoyancy forces. The vorticity associated with these stresses, which is of the same order v_v/l_v in the thermal plume and in the outer viscous region, diffuses outwards and downwards against the generated flow; this is thus governed by the Navier–Stokes equations with a Reynolds number of $v_v l_v/\nu = 1$. Then, $l_v/l_h = Pr$ because $v_v = v_h$ and $v_h l_h/\alpha = 1$.

In the thermal plume the transverse variations of the velocity are of order $\delta_t v_v/l_v$, small compared with the velocity $u_0'(x')$ in the centreplane of the plume, which by continuity must be of order v_v. When evaluating these changes, we can use the following simplified form of the momentum equation in the vertical direction:

$$g\beta(T - T_\infty) + \nu \frac{\partial^2 u'}{\partial y'^2} = 0, \tag{4.1}$$

where we have left out the convective terms and the term associated with the variation of the pressure from the external hydrostatic pressure. These terms, of order v_v^2/l_v, are smaller by the factor δ_t/l_v than the characteristic value, $\nu v_v/l_v\delta_t$, of the viscous term in (4.1).

In the thermal plume the temperature distribution satisfies, for $x' > 0$, the equation

$$u_0'(x')\frac{\partial T}{\partial x'} - y'\frac{\mathrm{d}u_0'}{\mathrm{d}x'}\frac{\partial T}{\partial y'} = \frac{\nu}{Pr}\frac{\partial T}{\partial y'^2}, \tag{4.2}$$

where $u_0'(x')$ is to be determined from the matching conditions with the outer viscous region. From (4.2) we can derive the relation $\delta_t^2 \sim \nu l_v/v_v Pr$, or $\delta_t/l_v \sim Pr^{-1/2}$, for the thickness δ_t of the thermal plume. Equation (4.2) must be solved with the conditions $T = T_\infty$ at $y' \to \pm\infty$, $\partial T/\partial y' = 0$ at $y' = 0$, and

$$u_0'(x')\int_{-\infty}^{\infty} \rho c_p (T - T_\infty)\,\mathrm{d}y' = q. \tag{4.3}$$

Notice that (4.1) and (4.3) lead to the result, obtained by Spalding & Cruddace (1961),

$$\left(\frac{\partial u'}{\partial y'}\right) = -\frac{g\beta q}{2\rho c_p \nu}\frac{1}{u_0'(x')} \tag{4.4}$$

for the vorticity, or velocity gradient, at the outer border of the the thermal plume. By equating the orders of magnitude of the two terms of (4.4), we obtain the relation $v_v^2/l_v = g\beta q/\rho c_p \nu$, which together with the relations $v_v = v_h$ and $l_v = l_h Pr$, given before, leads to

$$v_v = v_h = (\alpha g\beta q/\lambda_\infty)^{1/3}, \quad l_v/Pr = l_h = (g\beta q/\lambda_\infty \alpha^2)^{-1/3}, \tag{4.5}$$

where v_h and l_h are identical to those obtained before for the case when $Pr \sim 1$, given in (2.1).

When the coordinates are measured with l_v and the velocity with v_v, the governing equations for the non-dimensional vorticity and stream function in the outer viscous region, where $T = T_\infty$, take the form

$$-\hat{\omega} = \frac{\partial^2 \hat{\psi}}{\partial \hat{r}^2} + \frac{1}{\hat{r}}\frac{\partial \hat{\psi}}{\partial \hat{r}} + \frac{1}{\hat{r}^2}\frac{\partial^2 \hat{\psi}}{\partial \varphi^2}, \tag{4.6}$$

$$\frac{1}{\hat{r}}\left(\frac{\partial \hat{\psi}}{\partial \varphi}\frac{\partial \hat{\omega}}{\partial \hat{r}} - \frac{\partial \hat{\psi}}{\partial \hat{r}}\frac{\partial \hat{\omega}}{\partial \varphi}\right) = \frac{\partial^2 \hat{\omega}}{\partial \hat{r}^2} + \frac{1}{\hat{r}}\frac{\partial \hat{\omega}}{\partial \hat{r}} + \frac{1}{\hat{r}^2}\frac{\partial^2 \hat{\omega}}{\partial \varphi^2} \tag{4.7}$$

in terms of $\hat{r} = r'/l_v = r/Pr$. These are the Navier–Stokes equations to be solved, in

the half-space $0 < \varphi \leqslant \pi$, with the boundary conditions

$$\hat{\psi} = \frac{1}{\hat{r}}\frac{\partial \hat{\psi}}{\partial \varphi}\hat{\omega} - \tfrac{1}{2} = 0 \quad \text{at} \quad \varphi = 0, \qquad \hat{\psi} = \hat{\omega} = 0 \quad \text{at} \quad \varphi = \pi, \tag{4.8}$$

and the condition that the vorticity $\hat{\omega}$ and velocity tend to zero for $\hat{r} \to \infty$, outside a viscous plume at $\varphi \ll 1$. No parameters are left in this problem, in which the flow is driven by the shear stresses at $\varphi = 0$. The solution has to be obtained numerically, after describing the singular structure of the solution for $\hat{r} \ll 1$ and $\hat{r} \gg 1$.

4.2. *Asymptotic description of the viscous region for large and small $\hat{r}$, and numerical solution of the viscous flow problem*

As first shown by Spalding & Cruddace (1961), for values of $\hat{r} \gg 1$ and sufficiently small φ, or, equivalently, for distances above the line source large compared with l_v, $\hat{\psi}$ takes the asymptotic self-similar form $\hat{\psi} = \hat{r}^{3/5} f(\hat{\xi})$, $\hat{\xi} = \varphi \hat{r}^{3/5}$ in the viscous layer bounding the thin thermal plume. Here $f(\hat{\xi})$ is given by $5f''' + 3ff'' - (f')^2 = 0$, with the conditions $f(0) = f''(0)f'(0) + 1/2 = 0$ and $f'(\hat{\xi} \to \infty) = 0$. The numerical calculation – see also Kuiken & Rotem (1971) – yields $f(\infty) = 1.355$ and $f'(0) = 0.9334$. Thus, in the far field, outside the viscous plume, $\hat{\omega} = 0$ and $\hat{\psi}$ is given by the irrotational flow value

$$\hat{\psi} = f(\infty)\hat{r}^{3/5} \sin\left(3(\pi - \varphi)/5\right) / \sin\left(3\pi/5\right). \tag{4.9}$$

To obtain the appropriate boundary conditions for $\hat{r} \to 0$, we shall use the local Stokes approximation of (4.7), neglecting the convective terms. Taking into account the boundary conditions (4.8), solutions for the vorticity and stream function can be sought in the form

$$\hat{\omega} = D(\pi - \varphi) + \omega', \qquad \hat{\psi} = U_0 \hat{r} \sin\varphi + \psi', \tag{4.10}$$

where $\omega' \to 0$ and $\psi'/\hat{r} \to 0$ when $\hat{r} \to 0$. The linearized form of (4.8) leads, for $\hat{r} \to 0$, to the relation $D = 1/2\pi U_0$. The leading terms of the expansion of $\hat{\psi}$ for small values of r are

$$\hat{\psi} = (U_0\hat{r} - \tfrac{2}{3}D\hat{r}^2 + \ldots)\sin\varphi + (-\tfrac{1}{4}D\hat{r}^2 \ln\hat{r} + B_2\hat{r}^2 + \ldots)\sin 2\varphi + \ldots. \tag{4.11}$$

The constant U_0 corresponds to the vertical velocity at $\hat{r} = 0$, and $D = 1/2\pi U_0$ determines the leading term of the vorticity expansion in the vicinity of the source.

Equations (4.6)–(4.7) were solved numerically with the method used for the system (2.2)–(2.4). Taking into account (4.10) and (4.11), we can derive a mild form of the inner boundary conditions

$$\hat{r}\frac{\partial \hat{\omega}}{\partial \hat{r}} = \hat{r}\frac{\partial \hat{\psi}}{\partial \hat{r}} - \psi = 0 \qquad \text{at} \qquad \hat{r} \to 0, \tag{4.12}$$

while at $\hat{r} = \hat{r}_{max}$, we use for $\hat{\psi}$ a composite expression, based on the self-similar plume solution $\hat{r}^{3/5} f(\hat{\xi})$ and (4.9).

It can be observed that no parameter is left in the hydrodynamic system of equations (4.6)–(4.7) and in the above boundary conditions. The results of the calculations are presented in figures 7 and 8; the isovorticity lines and the streamlines are shown in figure 7, and the vertical velocity, $u_0(\hat{x})$, at the centreplane of the plume, $\hat{y} = 0$, is shown in figure 8 with a solid line. At the line source, $\hat{r} = 0$, the velocity is $U_0 = 0.87$. The centreplane velocity approaches for large $\hat{x}$ the well-known self-similar asymptotic form $f'(0)\hat{x}^{1/5}$, which is shown with circles in figure 8 together with the asymptotic value $0.5706 f(\infty)(-\hat{x})^{-2/5}$, below the line source, shown with triangles.

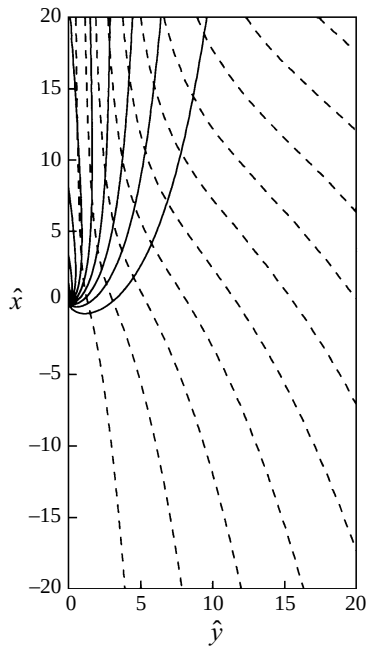

FIGURE 7. Computed streamlines (dashed lines, $\hat{\psi}$ at intervals of 1) and isovorticity lines (solid lines, $\hat{\omega}$ at intervals of 0.05) for $Pr = \infty$.

4.3. *Temperature in the vicinity of the source and in the thermal plume*

We can write the energy equation in the region $\hat{r} \sim 1/Pr$ near the source as

$$U_0 \frac{\partial \theta}{\partial \hat{x}} = \frac{1}{Pr} \hat{\Delta} \theta, \tag{4.13}$$

based on the uniform velocity U_0 given by (4.11) for $\hat{r} \to 0$, if terms of order $1/(Pr \ln Pr)$ are neglected. The solution of (4.13) with the condition $\theta \to 0$ at $\hat{r}Pr \to \infty$, and the condition (3.1) at $\hat{r}Pr \to 0$ is

$$2\pi\theta = \exp\left(\frac{Pr\, U_0 \hat{x}}{2}\right) K_0\left(\frac{Pr\, U_0 \hat{r}}{2}\right), \tag{4.14}$$

where K_0 is the modified Bessel function, behaving for $\hat{r}Pr = r \to 0$ as

$$2\pi\theta = \ln\left(4/U_0\right) - \gamma_E - \ln r, \tag{4.15}$$

where $U_0 = 0.87$ follows from the numerical calculation reported above and $\gamma_E = 0.577$ is Euler's constant. If we compare (4.15) with (3.2), we find that $A_0 = \ln 4/U_0 - \gamma_E = 0.948$. This value of A_0 is very close to the value obtained numerically for $Pr = 10$ and, surprisingly, also very close to the value of A_0 obtained for all the other values of the Prandtl number.

The solution of the problem (4.6)–(4.8) provides the dimensionless velocity $u_0(\hat{x})$, which then can be used to solve the problem (4.2)–(4.3) for the thermal plume. Equation (4.2), when written in terms of the variables

$$\psi = \hat{y} u_0(\hat{x}), \qquad \zeta = \frac{1}{Pr} \int_0^{\hat{x}} u_0(z)\, \mathrm{d}z, \tag{4.16}$$

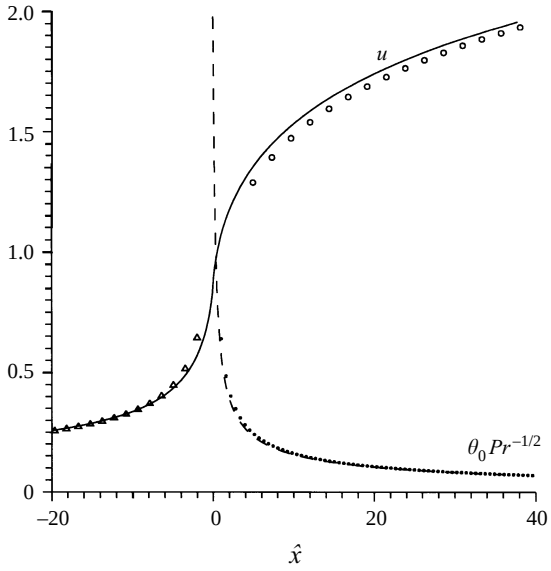

FIGURE 8. Computed vertical velocity (solid line) and temperature (dashed line) at the centreplane of the plume for $Pr = \infty$. The asymptotic description is also given for the temperature and velocity above the source (with dots and circles) and the velocity below the source (with triangles).

takes the form $\theta_\zeta = \theta_{\psi\psi}$. The solution, with the initial condition $\theta = \delta(\psi)$ at $\zeta = 0$, is

$$\theta = \frac{1}{(\pi\zeta)^{1/2}} \exp(-\psi^2/4\zeta), \tag{4.17}$$

and the centreplane temperature $\theta_0(\hat{x})$, for $\hat{x} \sim 1$, is given by

$$\theta_0(\hat{x}) Pr^{-1/2} = \pi^{1/2} \left(\int_0^{\hat{x}} u_0(z)\, \mathrm{d}z \right)^{-1/2}, \tag{4.18}$$

plotted in figure 8 with a dashed line. This is to be compared with the asymptotic self-similar value $\theta_0 Pr^{-1/2} = (5\pi f'(0)/6)^{-1/2} \hat{x}^{-3/5} = 0.6397 \hat{x}^{-3/5}$, shown also with a dotted line in figure 8, corresponding to a thermal boundary layer of thickness of order $l_h Pr^{1/10} (x'/l_h)^{2/5}$, which is $Pr^{-1/2}$ smaller than the thickness of the viscous plume.

5. Free convection heat transfer from wires at small and finite Grashof numbers

5.1. *Formulation and numerical description for* $Gr \sim 1$, $Pr \sim 1$

We shall describe in this Section the steady laminar free convection flow around horizontal thin wires, posing the problem so as to find the uniform surface temperature, T_w, of the wire that leads to a given heat flux q per unit length. The analysis will also be applicable to the description of the flow and heat transfer around inclined wires if g is replaced by the component g_n of g normal to the wire axis.

The problem was formulated in non-dimensional form in § 2 as to find the solution of (2.2)–(2.6), calculating the wire temperature θ_w, and therefore the Nusselt number, $Nu = 1/2\pi\theta_w$, as a function of Pr and the non-dimensional value $\varepsilon = a/l_h$ of the radius of the wire.

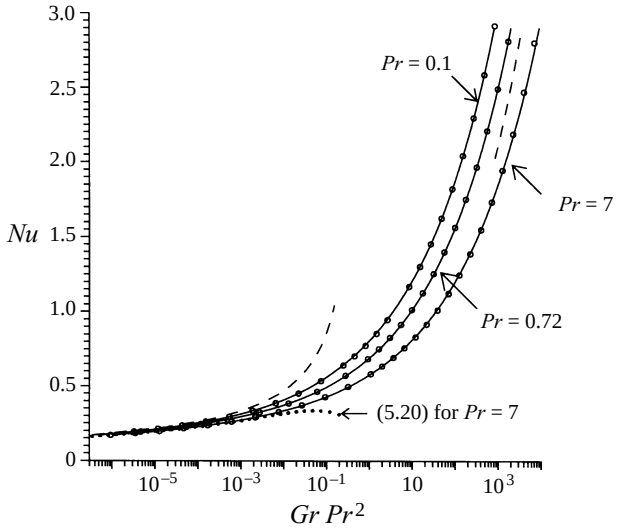

FIGURE 9. Average Nusselt number as a function of $GrPr^2$: circles, numerical results; solid line, correlation formula (5.11); dashed line, asymptotic behaviour for small and large Gr and $Pr = 0.72$; dotted line, asymptotic formula (5.20) of large Prandtl and small Peclet, σ, numbers evaluated for $Pr = 7$.

For values of ε and Pr of order unity the problem has to be solved numerically. We use the numerical method described in § 2, ensuring that for large r the solution follows the asymptotic description given in (3.5) and (3.8), but replacing the conditions (3.9) by the conditions (2.6) at $r = \varepsilon$.

Calculations were carried out for a wide range of Gr, down to 10^{-6}. The resulting Nusselt numbers, for $Pr = 0.1$, 0.72 and 7, are shown in figure 9 with circles, as a function of $Gr\,Pr^2$, the appropriate parameter for the description of free convection flows at low Prandtl numbers. Examples of the form of the isotherms and streamlines are shown in figure 10 for $\varepsilon = 1$ and two values, 0.05 and 0.72, of Pr. Notice the recirculating region above the wire for $Pr = 0.05$.

A recirculating region is encountered, above the wire, for values of the Grashof number larger than a threshold value, shown in figure 3 with a dashed line, that depends on Pr. The height of the recirculating bubble, measured with a, and the angle of separation φ_b are shown in figure 11 for various values of Pr with solid and dashed lines, respectively. Notice that, at least for small Pr, the height of the bubble begins growing linearly with Gr, reaches a maximum and then decreases. This is due to the increasing role, when Gr grows, of the vertical buoyancy forces in the bubble region, which also cause the threshold value of Gr to grow to very large values when Pr is rising to values of order unity.

The emergence of the recirculating bubble is not the result of a real bifurcation, and the effects on the heat transfer are not significant close to the threshold value of Gr, because the bubble lies in the region where the convective effects are negligible, if $\varepsilon \lesssim 1$. The evolution of the structure of the recirculating bubble with increasing values of Pr is interesting, but will not be further analysed in this paper, although we shall give some additional details in Appendix A when looking at the limit $Pr \to 0$.

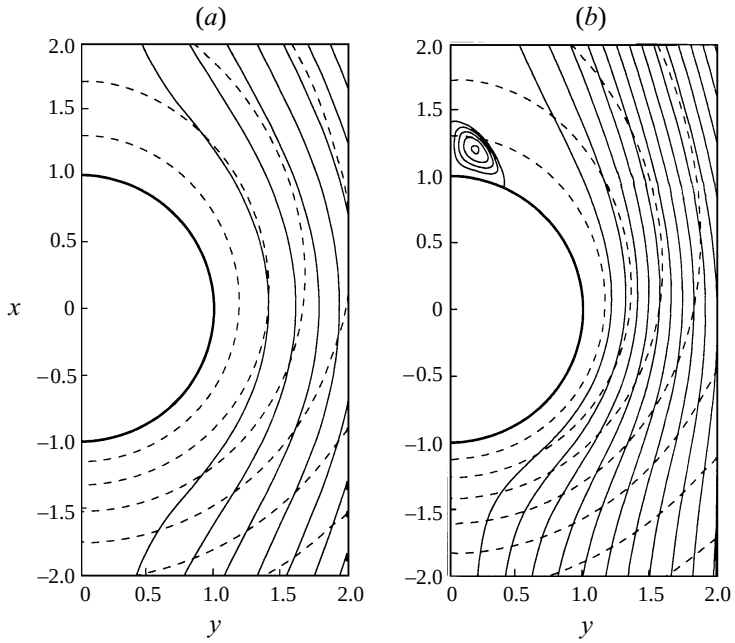

FIGURE 10. Computed streamlines around the cylinder for $\varepsilon = 1$ (solid lines, ψ at intervals of 0.1 outside the bubble, and 0.0002 inside) and normalized isotherms, $\tilde{\theta} = \theta/\theta_w$, (dashed lines, $\tilde{\theta}$ at intervals of 0.1): (*a*) $Pr = 0.72$, $\theta_w = 0.279$, (*b*) $Pr = 0.05$, $\theta_w = 0.247$.

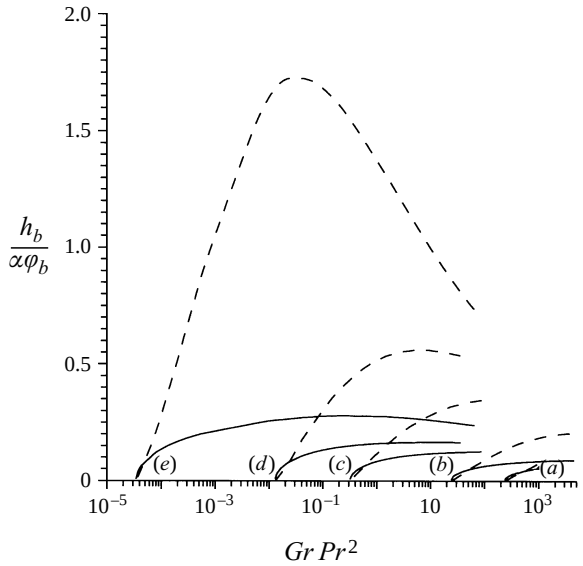

FIGURE 11. Computed height, h_b/a (dashed lines), and the separation angle, ϕ_b (solid lines), of the recirculating bubble; (*a*) $Pr = 0.3$, (*b*) $Pr = 0.2$, (*c*) $Pr = 0.1$, (*d*) $Pr = 0.05$, (*e*) $Pr = 0.01$.

5.2. *Heat transfer at* $Gr \ll 1$

For small values of Gr, $\varepsilon = a/l_h \ll 1$. Then, the flow field has two regions with disparate scales l_h and a. When seen with the scale l_h, the wire appears as a line source of heat. In an inner region, scaled with a, the effects of convection are

negligible, when compared with those of heat conduction and viscous transport of momentum.

If the local effects of convection are neglected for $r/\varepsilon \sim 1$, the temperature distribution will be given, for a wire of circular shape with non-dimensional radius ε, by the expansion

$$2\pi\theta = 2\pi\theta_w - \ln(r/\varepsilon) + \varepsilon B_1\{(r/\varepsilon) - (\varepsilon/r)\}\cos\varphi + \ldots. \tag{5.1}$$

In (5.1) we have included terms which are also solutions of the Laplace equation, involving negative powers of r, required to ensure that θ takes a constant value, θ_w, at the wire radius, $r = \varepsilon$. These terms will only produce changes of order ε in the outer temperature and flow fields. The small local effects of convection will modify (5.1) with terms of order $\varepsilon/\ln\varepsilon$; which, again, do not affect the outer region in first approximation.

If we anticipate that for $\delta = -1/\ln\varepsilon \ll 1$ we can neglect the effect on the outer buoyant flow of the momentum sink associated with the drag of the wire, we can derive the relation

$$2\pi\theta_w = Nu^{-1} = -\ln\varepsilon + A_0(Pr) \tag{5.2}$$

obtained from the requirement that the distributions (5.1) and (3.2) coincide in the intermediate region $\varepsilon \ll r \ll 1$. This relation, together with (2.7), determines the Nusselt number as a function of the Grashof number for small enough values of Gr, such that the perturbations of order δ left out of the right-hand side of (5.2) can be neglected.

In order to show this and how to obtain corrections of order δ to this Nusselt number, we analyse below the structure of the flow for $\varepsilon \ll 1$, but with ε not so extremely small as to allow us to neglect the perturbations of order $\delta \gg \varepsilon$. For this analysis we follow the procedure used by Tamada, Miuri & Miyagi (1983) and by Kropinski, Ward & Keller (1995), who consider $Re \ll 1$ but $-1/\ln Re$ of order unity in their analysis of the flow around cylinders (of arbitrary shape) at small Reynolds numbers.

We begin our analysis for small ε, with $\delta = -1/\ln\varepsilon$ of order unity, by describing the effect of the wire presence in the inner, $r \sim \varepsilon$, flow field. This field is given by an expansion in ε determined in lowest orders by the Stokes equations with the buoyancy forces evaluated using (5.1). This leads to the following small-r expansion for the stream function and the vorticity:

$$\psi = \left\{U\left(1 + \frac{1}{2\ln\varepsilon}\right)r + r^3\left(\frac{\ln r - 3/4}{32\pi Pr} - \frac{C}{8}\right) + E_1\frac{r\ln r}{\ln\varepsilon} + E_2\frac{\varepsilon^2}{r\ln\varepsilon}\right\}\sin\varphi, \tag{5.3}$$

$$\omega = \left\{-\frac{r\ln r}{4\pi Pr} + Cr - \frac{2E_1}{r\ln\varepsilon}\right\}\sin\varphi. \tag{5.4}$$

Two of the four constants appearing in the expansion (5.3) are determined by the requirement that ψ and ψ_r must be zero at $r = \varepsilon$. Thus we obtain

$$E_1 = -U + \varepsilon^2\frac{1 + 8\pi CPr\ln\varepsilon - \ln^2\varepsilon}{16\pi Pr(1 + 2\ln\varepsilon)}, \tag{5.5}$$

$$E_2 = -\frac{U}{2} + \varepsilon^2\frac{16\pi CPr(\ln\varepsilon - 2\ln^2\varepsilon) + (3\ln\varepsilon - 6\ln^2\varepsilon + 8\ln^3\varepsilon)}{128\pi Pr(1 + 2\ln\varepsilon)}. \tag{5.6}$$

We expect the remaining unknown constants, U and C, to be of order unity, as they are for a line source of heat. They must be obtained from the requirement that the inner expansion should match the outer expansion in the intermediate region $\varepsilon \ll r \ll 1$. However, for a pure line source of heat the outer field does not include the dipole source of vorticity, represented by the last term in (5.4), that we must include in the inner region, together with the last term of (5.3), to satisfy the boundary conditions on the wire. Hence, matching of the flow field near the wire and the outer field due to a pure line source of heat is not possible unless we include the effect on the outer flow field of the vorticity input from the wire, represented by the last term in (5.4), of order δ. Then, in order to account for this effect (or, equivalently, for the effect of the drag force on the wire due to the flow induced by the buoyancy forces) we must include in the small-r description (3.3), used for the line source of heat, the dipole term $-2E_1 \sin\varphi/r \ln\varepsilon$, and in (3.4) the corresponding term in the ψ description.

In summary, in order to calculate, up to terms of order ε, the outer temperature and flow fields due to gravity, associated with a heated thin circular wire, we should solve the Boussinesq equations (2.2)–(2.4), with the same far-field conditions (3.5) and (3.8) used for a line source of heat and the following behaviour for $\varepsilon < r \ll 1$:

$$2\pi\theta = -\ln r + A, \tag{5.7}$$

$$\omega = \left\{ -\frac{r \ln r}{4\pi Pr} + Cr + \frac{2U}{r \ln\varepsilon} \right\} \sin\varphi, \tag{5.8}$$

$$\psi = Ur \left\{ 1 - \frac{\ln r}{\ln\varepsilon} + \frac{1}{2\ln\varepsilon} \left(1 - \frac{\varepsilon^2}{r^2} \right) \right\} \sin\varphi. \tag{5.9}$$

The constants A, U and C appearing in these expressions must be calculated as part of the numerical solution for small or moderately small values of ε. The last term of (5.9) does not need to be included if the numerical calculations are carried out only for values of $r \gg \varepsilon$. However, the terms of order $-1/\ln\varepsilon$ should be retained, as if they were of order unity, unless ε is extremely small; notice that the drag force on the wire, $4\pi\rho\nu v_h U/\ln(1/\varepsilon)$, is small when compared with the vertical momentum flux in the outer region only due to the moderately small factor δ.

The numerical solution of the system (2.2)–(2.4), with the far-field description of the solution given in (3.5) and (3.8), and the small-r representation of (5.7)–(5.9), with the term in ε^2 left out of (5.9), should provide us with the temperature and flow field in the outer region, together with the constants A, C and U. These constants will then depend on the parameters Pr and $\delta = -1/\ln\varepsilon$ remaining in the formulation.

For $Pr \sim 1$ and small values of δ, we may expect the dependence of A, C and U on δ to be described by expansions in powers of δ – for example, $A(Pr, \varepsilon) = A_0 + \delta A_1(Pr) + \ldots$ – beginning with the values A_0, C_1 and U_0 for $\delta = 0$, to ensure matching, at $r \sim 1$, of θ, ω and ψ at $r \sim Pr$, with the line source of heat. The effect of the vorticity source, represented by the last term in (5.8) with $U = U_0$ in a first approximation, will introduce changes in A and U from A_0 and U_0 proportional to δ, for $\delta \ll 1$, which should be determined by a linear system of equations.

With A thus determined as a function of $\ln\varepsilon$ and Pr, the relation (5.7), namely

$$Nu^{-1} = -\tfrac{1}{3} \ln(2\pi Pr^2 GrNu) + A, \tag{5.10}$$

would allow us to calculate Nu as a function of Gr and Pr.

Pr	a_2	a_4	a_5	b
0.1	4.495	11.467	7.859	0.460
0.72	18.208	28.813	18.254	0.373
7	60.974	95.631	94.861	0.207

TABLE 2. The values of coefficients in the fitting formula (5.12).

5.3. *Correlation formula for* $Nu(Gr, Pr)$

Instead of using this procedure, we shall use the asymptotic form of (5.10) with $A = A_0$, for $GrPr^2 \to 0$, and the results of our numerical calculations, described in § 4.1, to obtain directly a correlation formula for the Nusselt number, valid for the steady laminar free convection flow for all Grashof number. This will be written in the form

$$GrPr^2 = \frac{1}{2\pi Nu} \exp\left(3A_0 - \frac{3}{Nu}\right) F(Nu, Pr) \tag{5.11}$$

which coincides with (5.10), for $GrPr^2 \to 0$, if $F \to 1$ for $Nu \to 0$.

For large Grashof numbers, when $Nu \gg 1$, F/Nu^5 should tend to a constant $a_5(Pr)$, chosen so as to obtain the well-known asymptotic relation, $Nu = b\,(Pr^2Gr)^{1/4}$, between Nu and Gr for free convection laminar flow for $Gr \gg 1$. The values of $b(Pr)$, shown in table 2, were obtained from the numerical solution, with a finite difference method, of the asymptotic boundary layer form of (2.2)–(2.4), given for example in Leal (1992). For $Pr \gg 1$, $b \to 0.435Pr^{-1/4}$, and if $Pr \ll 1$, $b \to 0.54$.

For $F(Nu, Pr)$ we use a polynomial correlation

$$F = 1 + a_2Nu^2 + a_4Nu^4 + a_5Nu^5, \tag{5.12}$$

where $a_5 = 2\pi \exp(3A_0)/b^4$, and the adjustable parameters a_2 and a_4, depending on the Prandtl number, are given in table 2. When (5.11) and (5.12) are used, with the approximately constant value 0.96 of A_0, the resulting Nusselt numbers, shown in figure 9 with solid lines, correlate, with errors lower than 1%, the values obtained from our numerical calculations, shown with circles in figure 9, of the free convection flow around heated wires in a wide range of Grashof numbers. We also show with dashed lines the asymptotic approximations, for $Gr \ll 1$, given by (5.11) with $F = 1$, and by $Nu = b(Pr^2Gr)^{1/4}$, for $Gr \gg 1$, respectively.

5.4. *Free convection heat transfer from thin wires at* $Pr \gg 1$

We shall describe here the free convection flow around wires of radius a small compared with $l_v = l_hPr = (g\beta q/\lambda_\infty \nu^2 Pr)^{-1/3}$, the characteristic size of the region around the wire where we find the vorticity generated by the baroclinic torques in the thermal plume, but not necessarily small compared with l_h. When for $\hat{\varepsilon} = a/l_v = \varepsilon/Pr \ll 1$ we look at the flow with scale l_v, the thin wire is seen as a line source of heat and a line sink of momentum (associated with the drag force on the wire by the flow generated by the buoyancy forces). Using the arguments of § 5.2, we can estimate as of order $-1/\ln\hat{\varepsilon}$ the errors introduced in the our analysis of the viscous region when we neglect the effects of the wire drag. Then, the flow in the outer viscous region is, in first approximation for $-1/\ln\hat{\varepsilon} \ll 1$, the one described in § 4, corresponding to a pure line source of heat. The vertical velocity induced at $\hat{r} \ll 1$ by buoyancy forces acting on the thermal plume is given by $U_0 = 0.87$, when measured with the scale v_h.

The arresting effect of the wire on this flow can be described using an analysis similar to that of Kaplun & Lagerstrom (1957) for the flow around cylinders at low Reynolds numbers, because, if we take into account that $v_h l_v/\nu = 1$, the effective Reynolds number, $U_0 v_h a/\nu = U_0\hat{\varepsilon}$, is small compared with unity. The flow field, at distances from the wire axis small compared with l_v, is described by the Stokes equations, and given by the stream function $\hat{\psi}$,

$$\hat{\psi}\ln(1/\hat{\varepsilon})/U_0\hat{\varepsilon} = \tilde{\psi} = \tilde{r}\left\{\ln\tilde{r} - \frac{1}{2}\left(1 - \frac{1}{\tilde{r}^2}\right)\right\}\sin\varphi, \tag{5.13}$$

written in terms of $\tilde{r}$, the radial distance scaled with a. The factor $U_0\hat{\varepsilon}/\ln(1/\hat{\varepsilon})$ is chosen to ensure matching, at $\tilde{r}\hat{\varepsilon} = \hat{r} \sim 1$, of the velocity U_0, given by the outer flow, to that given by the solution (5.13) of the Stokes equations in the inner region. We thus may expect errors of order $-1/\ln\hat{\varepsilon}$ in the velocity field given by (5.13), associated with the errors in the outer flow.

The temperature field is determined by the combined effects of convection, associated with the velocity field (5.13), and heat conduction. This leads to the energy equation

$$\tilde{v}_r\frac{\partial\tilde{\theta}}{\partial\tilde{r}} + \frac{\tilde{v}_\varphi}{\tilde{r}}\frac{\partial\tilde{\theta}}{\partial\varphi} = \frac{1}{\sigma}\left(\frac{\partial^2\tilde{\theta}}{\partial\tilde{r}^2} + \frac{1}{\tilde{r}}\frac{\partial\tilde{\theta}}{\partial\tilde{r}} + \frac{1}{\tilde{r}^2}\frac{\partial^2\tilde{\theta}}{\partial\varphi^2}\right), \tag{5.14}$$

where $\tilde{\theta} = \theta/\theta_w$, $\tilde{v}_r = \tilde{r}^{-1}\tilde{\psi}_\varphi$, $\tilde{v}_\varphi = -\tilde{\psi}_{\tilde{r}}$, to be solved, numerically, with the boundary conditions $\tilde{\theta} \to 0$ for $\tilde{r} \to \infty$ and $\tilde{\theta} = 1$ at $\tilde{r} = 1$. From the solution we calculate the Nusselt number

$$Nu = -\frac{1}{2\pi}\int_0^{2\pi}\tilde{r}\frac{\partial\tilde{\theta}}{\partial\tilde{r}}\bigg|_{\tilde{r}=1}\mathrm{d}\varphi \tag{5.15}$$

as a function of the effective Péclet number

$$\sigma = U_0 Pr\hat{\varepsilon}/\ln(1/\hat{\varepsilon}) = (U_0 Pr v_h a/\nu)/\ln(\nu/v_h a). \tag{5.16}$$

Values of σ of order unity correspond to the distinguished regime in which, for large Prandtl numbers, the size of the heated region around the wire, under forced flow with the small Reynolds number $U_0\hat{\varepsilon}$, is of the order of its radius and, then, $Nu \sim 1$. The Nusselt numbers resulting from our the calculations are shown, with a solid line, in figure 12; where we also include the asymptotic representations of $Nu(\sigma)$ for large and small values of σ to be given below. We should expect errors of order $-1/\ln\hat{\varepsilon}$ due to the errors in (5.13).

For $\sigma \gg 1$ heat conduction effects are confined to a thin thermal boundary layer around the wire, which becomes the thermal plume above. The temperature distribution in the boundary layer can be described by the expansion

$$\tilde{\theta} = \tilde{\theta}_0 + \sigma^{-1/3}\tilde{\theta}_1 + \ldots, \tag{5.17}$$

where $\tilde{\theta}_0$ and $\tilde{\theta}_1$ are functions of the boundary layer variables φ and $\zeta = \sigma^{1/3}(\tilde{r} - 1)$, given by linear equations. These were solved numerically to calculate the Nusselt number,

$$Nu = c_0\sigma^{1/3} + c_1 + \ldots, \tag{5.18}$$

where

$$c_0 = -\frac{1}{\pi}\int_0^\pi\frac{\partial\tilde{\theta}_0}{\partial\zeta}\mathrm{d}\varphi = 0.579, \qquad c_1 = -\frac{1}{\pi}\int_0^\pi\frac{\partial\tilde{\theta}_1}{\partial\zeta}\mathrm{d}\varphi = 0.0917. \tag{5.19}$$

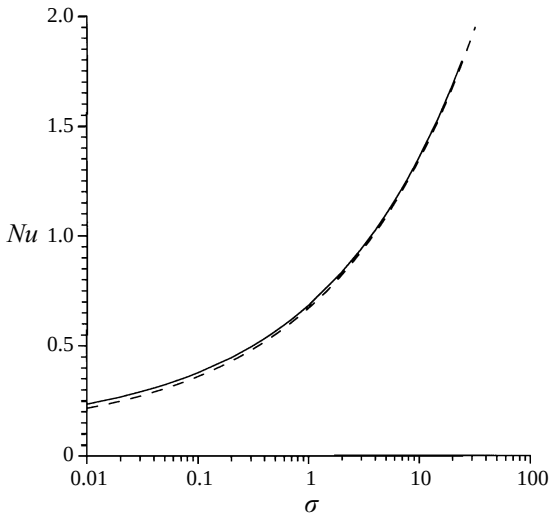

FIGURE 12. Computed average Nusselt number as a function of the effective Péclet number σ (solid line); dashed lines, two-term asymptotic expansion (5.18) for large σ.

The two-term expansion (5.18), represented in figure 12 with a dashed line, describes unexpectedly well the numerical results for values of $\sigma > 0.5$.

For small values of σ, the size of the heated region is $\tilde{r}_c \gg 1$. Then, the solution of (5.14) is well approximated by the solution $\tilde{\theta} = 1 - Nu \ln \tilde{r}$ of the Laplace equation for $\tilde{r} \sim 1$, but no longer where $\tilde{r}$ becomes of order $\tilde{r}_c$, to be determined below, when convective effects must be taken into account. The value of $\tilde{r}_c$ depends, for a given $\hat{\varepsilon}$, on Pr. We shall proceed, as Hieber & Gebhart (1968) did for the forced flow case, by considering the distinguished regime $\hat{\varepsilon} \ll 1$ and $1/Pr = \hat{\varepsilon}^m$ with $0 < m < 1$. Then, it is easy to see that convective effects balance conduction at distances $\tilde{r} \sim \tilde{r}_c = 1/\hat{\varepsilon} Pr \gg 1$, where the velocity, according to (5.13), is uniform, given by $v_h U_0(1-m)$ with errors of order $-1/\ln \hat{\varepsilon}$. We can describe the temperature distribution using the solution of the Oseen equation, with the velocity $U_0 v_h(1-m)$, and the condition $\tilde{\theta} = 1 - Nu \ln \tilde{r}$ for small $\tilde{r}$. Then we obtain for the Nusselt number

$$Nu = \left[-\ln(\hat{\varepsilon} Pr) + 0.948 - \ln\left(1 - \frac{\ln Pr}{\ln(1/\hat{\varepsilon})}\right)\right]^{-1}, \tag{5.20}$$

where the constant $0.948 = A_0 = \ln(4/U_0) - \gamma_E$. This is valid, with errors of order $1/\ln \sigma^{-1}$, for $Pr \gg 1$ and $\varepsilon \ll 1$, and coincides with (5.2) for $Pr \sim 1$, when $\ln Pr \ll \ln(1/\hat{\varepsilon})$, if we retain the variation of A_0 with Pr. Equation (5.20) has been plotted in figure 9, with a dotted line, for $Pr = 7$.

6. Conclusions and generalization

The main objective of this paper is the description of the steady laminar free convection flow and heat transfer from heated wires at small Grashof numbers. The problem was posed as to find the temperature of the wire T_w leading to a given heat loss q, per unit time and length of the wire, assumed to be infinitely long. The Boussinesq form of the equations was used, and when written in non-dimensional form, using the scales $T_h - T_\infty$, l_h and v_h given in (2.1), only two parameters are left

in the problem: $\varepsilon = a/l_h$ and Pr. The Nusselt number, $Nu = q/2\pi\lambda_\infty(T_w - T_\infty)$, is then a function of ε and Pr.

The buoyancy forces are confined to the heated region around the wire, of size $l_h = (\lambda_\infty\alpha^2/g\beta q)^{1/3}$ if ε is not large compared with 1, and to the thermal plume above. The transport of vorticity due to viscous effects is confined to the region around the wire of size $l_v = Prl_h$, if $\hat{\varepsilon} = a/l_v$ is not large compared with 1, and to the viscous plume above. The sketch in figure 2 gives the relative position of these regions for $Pr \ll 1$ and $Pr \gg 1$.

When ε and $\hat{\varepsilon} = \varepsilon/Pr$ are both small compared with 1, the wire appears to act as a pure line source of heat, when we observe the temperature and flow fields with the scale l_h. These fields are described in terms of the numerical solution of the non-dimensional Boussinesq equations for the line heat source in § 3, for values of order unity of the single parameter Pr, in § 4 for $Pr \gg 1$ and in Appendix A for $Pr \ll 1$. Two important constants, U_0 and A_0, of order unity, are encountered in the description of the velocity and temperature fields near the source; they are given in table 1 for various values of Pr.

When $\varepsilon^3 = a^3g\beta q/\lambda_\infty\alpha^2 \ll 1$, the heat transfer around circular wires is determined by the relation (5.2), obtained by extending to the wire surface the near-source distribution of the temperature field around the line heat source. This asymptotic relation for the inverse of the Nusselt number is valid only for very small values of the Grashof number, or more precisely for small values of ε, because terms of order $\delta = 1/\ln\varepsilon^{-1}$ have been neglected. Notice that ε^3 is the main parameter determining the Nusselt number for values of the Grashof number such that $\varepsilon \ll 1$. In the parameter plane (Gr, Pr), shown in figure 3, the line $\varepsilon = 1$ corresponds, roughly, to the line $GrPr^2 = 1$.

The non-dimensional velocity U_0 at the line source, determines, in first approximation, the flow around the wire. This flow is given by the Stokes equations if the effective Reynolds number, $U_0\hat{\varepsilon} = U_0\varepsilon/Pr$, based on U_0v_h and the radius of the wire, is small compared with unity. This is the case if $\hat{\varepsilon} \ll 1$; then we find a drag force, $4\pi\rho\nu v_hU_0/\ln\hat{\varepsilon}^{-1}$, on the wire, whose effect on the outer flow appears as a line sink of momentum, counteracting the momentum generated by the buoyancy forces. If $1/\ln\hat{\varepsilon}^{-1} \ll 1$ the effect of this momentum sink can be neglected when describing the outer flow.

For $Pr \gg 1$ the size, l_h, of the heated region around the line source or wire and the thickness of the thermal plume above are small compared with the size, $l_v = Prl_h$, of the viscous region, where we find the vorticity generated by the buoyancy forces in the thermal plume. In § 4 we calculated, for $\hat{\varepsilon} \ll 1$, the flow velocity, $U_0v_h = 0.87v_h$, at the line source and the apparent temperature $A_0(T_h - T_0) = 0.95q/\lambda_\infty$. In § 5 we show how to calculate the flow and temperature fields around the wire in the distinguished limiting case when the Reynolds number associated with the buoyant flow is $\hat{\varepsilon} = a/l_v \ll 1$, but the effective Péclet number $\sigma = U_0\hat{\varepsilon}Pr/\ln\hat{\varepsilon}^{-1}$ is of order unity; then, the size of the heated region around the wire is of order a. The dependence of the Nusselt number on σ is shown in figure 12, where we also plot the values of Nu given by the two term asymptotic expansion for $\sigma \gg 1$. The analysis of the thermal boundary layer for large σ fails when $\hat{\varepsilon}$ becomes of order unity because the flow is no longer given by the Stokes description of (5.13). For larger values of $\hat{\varepsilon}$, the local buoyancy forces should be included in the description of the thermal boundary layer.

As indicated in Appendix A, for small values of the Prandtl number viscous effects in the free convection flow around thin wires, or induced by line heat sources, are confined to a region of size l_hPr around the wire, or heat source, and to a thin layer

above. The structure of the flow around the wire depends on the effective Reynolds number $Re = U_0\varepsilon/Pr = 1.05\hat{\varepsilon}$, and we may find a recirculation region above the wire – and for small Pr perhaps also unsteady effects – for values of Re larger than critical values. The threshold value of ε, and therefore of the Grashof number, for the appearence above the wire of a recirculating region depends on Pr; it becomes very large when Pr is of order unity or larger and must be given by $Re_c Pr/1.05$ when $Pr \to 0$. Here Re_c, approximately 3.15, is the value of the Reynolds number, based on a, for the appearance of a recirculating region in the wake of a circular cylinder under a forced flow with constant density. No more details will be given in this paper of the change in the near-wake flow structure with Pr and Gr, aside from showing in figure 3, with a dashed line, the threshold values of $Gr(Pr)$ for the appearance of a recirculating bubble, and giving in figure 11 the size of the bubbles.

Non-Boussinesq effects can be neglected in the outer region if $q/\lambda_\infty T_\infty \ll 1$, so that the characteristic temperature rise above the ambient, of order q/λ_∞ in this region, is small compared with T_∞. Even if this condition is satisfied, we are forced to account for non-Boussinesq effects in the inner region, when $\varepsilon \ll 1$, if the value of the non-dimensional wire temperature rise $(T_w - T_\infty)/T_\infty$, or $q/\lambda_\infty T_\infty 2\pi\delta$, is no longer small compared with unity. These effects on the inner temperature distribution can be easily taken into account because this temperature is not affected, in first approximation, by the convective effects, so that we only need to account for the variation of the heat conductivity, λ, with the temperature. Thus, in the inner region we have to solve the heat conduction equation $\nabla \cdot (\lambda \nabla T) = 0$, which can be written as the Laplace equation $\Delta\Theta = 0$ for the function $\Theta = \int_{T_\infty}^{T} (\lambda(T')/\lambda_\infty)\,\mathrm{d}T'/T_\infty$. This equation must be solved with the condition $\Theta = \Theta_w$ in the cylinder surface and the far-field condition

$$(r'\Theta_{r'})|_{r'\to\infty} = -q/2\pi\lambda_\infty T_\infty, \tag{6.1}$$

where r' is the dimensional radial coordinate. For a circular cylinder of radius a the inner temperature distribution is then given by

$$\Theta - \Theta_w = -(q/2\pi\lambda_\infty T_\infty)\ln(r'/a), \tag{6.2}$$

where the factor $q/2\pi\lambda_\infty T_\infty$ is assumed to be small compared with 1. The relation (6.2), giving the temperature distribution for $r'/a \ll l_h/a$, should match with the temperature distribution of the outer region given, for $r'/l_h \ll 1$, by

$$\Theta = (q/2\pi\lambda_\infty T_\infty)(-\ln(r'/l_h) + A_0), \tag{6.3}$$

so that we obtain the relation

$$\Theta_w = \int_{T_\infty}^{T_w} \{\lambda(T')/\lambda_\infty\}\,\mathrm{d}T'/T_\infty = (q/2\pi\lambda_\infty T_\infty)\{\ln(l_h/a) + A_0(Pr)\} \tag{6.4}$$

to calculate T_w in terms of q. This description of the effects of variable properties in the temperature field follows the analysis given by Hodnett (1969) for the low-Reynolds-number forced flow around cylinders, and it can be similarly extended to describe the effects on the free convection flow field.

The relation (6.4) is valid for a cylinder of non-circular shape if a is replaced by the effective radius a_e, when this turns out to be small compared with l_h. In this case, Θ is also given in the inner region by the Laplace equation, $\Delta\Theta = 0$, the condition $\Theta = \Theta_w$ on the cylinder surface, and the far-field condition (6.1). The solution of this linear problem leads to a distribution of $(\Theta - \Theta_w)\lambda_\infty T_\infty/q$ depending only on the

cylinder shape. For large r',

$$\Theta - \Theta_w = -(q/2\pi\lambda_\infty T_\infty)\ln(r'/a_e), \tag{6.5}$$

where a_e must be obtained as part of the solution. This inner heat conduction problem can be solved in closed form using the method of conformal transformation for a variety cylindrical shapes. This is the case for cylinders of elliptical shape, for which $a_e = (a_1 + a_2)/2$ in terms of the values a_1 and a_2 of the semi-axes.

This research has been supported by the Spanish DCICYT, under Contract No PB 94-0400, and by INTA, under Contract No 4070-0036/1996. V.N.K. would like to express his gratitude to the DGICYT for a postdoctoral fellowship at UP Madrid.

Appendix A. The limiting case of $Pr \to 0$

In this Appendix we begin by considering the flow in the vicinity of the line heat source in the inviscid limit $Pr \to 0$. Later, we shall deal with the description of the flow field around thin wires when $Pr \ll 1$.

For the line source of heat, the temperature field is given, in first approximation, for $r \ll 1$, by the radially symmetric solution $2\pi\theta = A_0 - \ln r$ of the Laplace equation. Then, for $Pr = 0$ and $r \ll 1$ the equation (2.3) of the vorticity is simplified to

$$v_r \frac{\partial \omega}{\partial r} + \frac{v_\varphi}{r}\frac{\partial \omega}{\partial \varphi} = \frac{\sin\varphi}{2\pi r}. \tag{A 1}$$

For small r, we shall write the solution of (A 1) and $\Delta\psi = -\omega$ in the form

$$\psi = U_0 r \sin\varphi + \psi', \qquad \omega = D(\pi - \varphi) + \omega', \tag{A 2}$$

where $\psi'/r \to 0$ and $\omega' \to 0$ when $r \to 0$. From the linearized form of (A 1), we obtain $D = 1/2\pi U_0$. For $r \ll 1$, ω' and ψ' are given by the linear system

$$U_0 \cos\varphi \frac{\partial \omega'}{\partial r} - U_0 \sin\varphi \frac{1}{r}\frac{\partial \omega'}{\partial \varphi} = -\frac{D}{r}\frac{\partial \psi'}{\partial r}, \tag{A 3}$$

$$\Delta\psi' = -D(\pi - \varphi) - \omega'. \tag{A 4}$$

The leading terms of the expansion for small r of the solution of (A 3)–(A 4) can be written as

$$\psi' = -\frac{r^2}{3\pi U_0}\sin\varphi + \left(B_2 r^2 - \frac{r^2 \ln r}{8\pi U_0}\right)\sin 2\varphi + \ldots, \tag{A 5}$$

$$\omega' = \frac{r\sin\varphi}{3\pi^2 U_0^3}\ln\left(\frac{\sin\varphi}{1-\cos\varphi}\right) + \left\{B_1 r + \left(-\frac{2B_2}{\pi U_0^2} + \frac{1}{8\pi^2 U_0^3}\right) r\ln r + \frac{r\ln^2 r}{8\pi^2 U_0^3}\right\}\sin\varphi + \ldots, \tag{A 6}$$

where the constants U_0, B_1 and B_2 must be obtained as part of the numerical solution of the general inviscid line heat source problem. Up to the terms retained above, the vorticity maintains, for $x > 0$, the constant values $\omega = 1/2U_0$ at $y = 0+$, and $\omega = -1/2U_0$ at $y = 0-$. Notice that the last term of (A 5) leads to an infinite value of the vertical velocity gradient at $r = 0$, in agreement with the large values obtained numerically for small Pr, shown in figure 5.

In the inviscid limit, $Pr \to 0$, the vorticity equation (2.3) indicates that these opposite values will also be constant for all positive values of $x \sim 1$ at $y = 0+$ and $y = 0-$, where $\partial\theta/\partial y = 0$. Viscous effects will obviously provide, for non-zero values of Pr, a smooth transition between these values. This result, given by the inviscid analysis, of constant values $\pm 1/2U_0 \approx 0.48$ of the vorticity on the two faces of the centreplane above the line source, is in contrast with the infinite value that the inviscid self-similar plume solution gives at $y = 0\pm$. As shown by Kuiken & Rotem (1971), the solution of (3.6) and (3.7) for $Pr = 0$ leads to a value of the vorticity $\omega = -0.61 r^{-1/5}\xi^{-1/3}$ for $\xi \ll 1$. Viscous effects acting on a layer of thickness $\xi \sim Pr^{1/2}$ bound the vorticity to peak values of order $r^{-1/5}Pr^{-1/6}$. For the transition from the peak initial value of the vorticity, of order unity, to these values we thus may expect to need a length of order $Pr^{-5/6}$ to reach the self-similar viscous structure. However, the entrainment velocity of the outer irrotational flow comes from the buoyancy forces in the thermal plume, and it is given well by the asymptotic relation $v_e = -0.909 r^{-2/5}$. As a consequence, the velocity distribution below the source is seen in figure 5 to approach rapidly the irrotational asymptote $u = 0.956(-x)^{-2/5}$ for $(-x) \gg 1$ and $Pr = 0$.

In summary, for small Prandtl numbers the line heat source leads to a temperature field near the source determined by the constant $A_0 = 0.97$ and a flow velocity at the source $U_0 v_h = 1.05 v_h$. When we want to describe the temperature and velocity fields around thin wires, with $\varepsilon = a/l_h \ll 1$, we can use, as we did in the main text for $Pr \sim 1$, the line heat source solution by extending the validity, if the wire is circular, of the near-source temperature distribution, $2\pi\theta = A_0 - \ln r$, to the wire surface, $r = \varepsilon$, and thus determine the Nusselt number from the relation $Nu^{-1} = 2\pi\theta_w = 0.97 - \ln\varepsilon$.

The flow field around the wire is determined by the velocity $U_0 v_h = 1.05 v_h$, which we would obtain at the line source of heat, induced by the buoyancy forces acting on the heated region. The structure of this flow near the wire depends on the effective Reynolds number, $Re = U_0\varepsilon/Pr$, based on the velocity $U_0 v_h$ and the wire radius. When $\hat{\varepsilon} = \varepsilon/Pr$ is of order unity the flow around the wire should be described using the constant-density Navier–Stokes equations, without buoyancy forces. In particular, the vertical force per unit length on the wire is $c_D a\rho(U_0 v_h)^2$, where the drag coefficient is a function of the Reynolds number, of order unity if ε/Pr is of order unity or large. In any case, the effect of the momentum sink represented by this drag on the buoyancy-induced momentum flux, which is of order $\rho v_h^2 l_h$ in the region $r \sim l_h$ around the wire, can be neglected because $a \ll l_h$.

It is interesting to observe how the structure of the flow around thin wires at small Prandtl numbers changes with the value of the Reynolds number, $Re = 1.05\hat{\varepsilon}$, of the generated forced flow. If $Re > 3.14$ we find (according to our numerical calculations for the forced flow around cylinders) a recirculation region above the wire. The relations $Gr = \varepsilon^3/2\pi NuPr^2$ and $Nu^{-1} = 0.97 - \ln\varepsilon$ and the condition $\varepsilon_c/Pr = 2.99$ lead to $Gr_c = 4.26Pr(0.97 - \ln(2.99Pr))$, shown in figure 3 with a dotted line. For $Pr \ll 1$ and values of Re larger than a second critical value, about 20, which cannot be calculated with our numerical scheme, the flow around the wire may be expected to become oscillatory, as is the case for forced flow around wires.

Appendix B. Inclined line source

In this Appendix we consider the effects of the inclination with respect to the horizontal of an infinitely long line source of heat. For the description of the flow we shall use a coordinate z in the direction of a non-vertical line source and two coordinates, x and y, to characterize the points in planes normal to the line source,

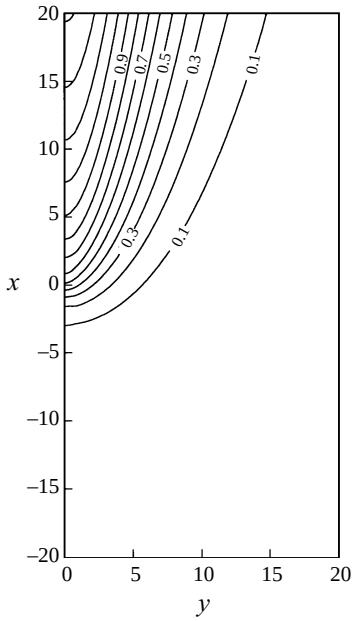

FIGURE 13. Computed isolines of axial velocity $\tilde{w}$ for natural convection around an inclined infinitely long line source of heat, for $Pr = 0.72$.

at $x = y = 0$. The components of the acceleration due to gravity with respect to this coordinate system are $(-g_n, 0, -g_l)$.

The translation invariance of the problem with respect to the coordinate z implies that θ and the velocity components (u, v, w) are functions only of the coordinates x and y. The temperature and velocity components u and v are given by the analysis of § 2, with g replaced by g_n when determining the velocity and length scales v_h and l_h. The velocity component w is given by the non-dimensional equation

$$v_r \frac{\partial w}{\partial r} + \frac{v_\varphi}{r} \frac{\partial w}{\partial \varphi} = Pr \Delta w + \theta \tan \phi. \tag{B 1}$$

Here v_r and v_φ are given by the solution (2.2)–(2.4), and $\tan \phi = g_l / g_n$ is determined by the angle of inclination $\phi < \pi/2$ of the line source with respect to the horizontal. Due to the linearity of (B 1), the function $\tilde{w} = w / \tan \phi$ is independent of ϕ.

In the vicinity of the line source, for small values of r, the normalized velocity $\tilde{w}$ is determined by the Stokes equation, obtained from (B 1) by neglecting the convective terms. Taking into account (3.2), we can write

$$\tilde{w} = \tilde{w}_0 + \frac{r^2}{8\pi Pr} \{\ln r - (1 + A_0)\} + G_1 r \sin \varphi + G_2 r^2 \sin 2\varphi + \ldots, \tag{B 2}$$

where the constants appearing in this small-r expansion must be obtained as part of the numerical solution of (B 1). The constant $\tilde{w}_0$ determines the value of the z velocity component at the line source.

Equation (B 1) was solved numerically, with the method used for the system (2.2)–(2.4), with the boundary condition

$$r \frac{\partial \tilde{w}}{\partial r} = 0 \qquad \text{at} \qquad r \to 0, \tag{B 3}$$

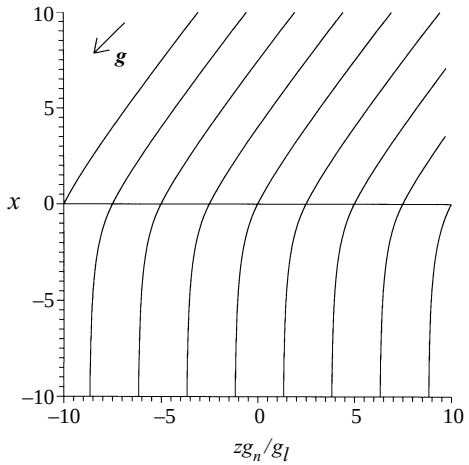

FIGURE 14. Streamlines in the vertical plane for the inclined infinitely long line source, with $Pr = 0.72$.

while for $r \to \infty$ we require

$$\tilde{w} = 0 \quad \text{for} \quad \pi/6 < \varphi < \pi; \qquad \frac{\partial \tilde{w}}{\partial r} = 0 \qquad \text{for} \quad 0 < \varphi < \pi/6. \tag{B 4}$$

The isolines of $\tilde{w}$ are shown in figure 13 for $Pr = 0.72$; $\tilde{w}_0 = 0.48$. In figure 5 we show, with a dotted line, also for $Pr = 0.72$, how $\tilde{w}$ varies with x in the vertical plane of the line source. In the thermal plume, for $x \gg 1$, where the effects of the pressure gradient disappear in first approximation, the functions $\tilde{w}$ and u become self-similar, and are given by the same equations with the same boundary conditions; hence, $\tilde{w}/u \to 1$ when $x \to \infty$, but the convergence is slow. Below the line source, $\tilde{w}$ decreases rapidly to 0.

The streamlines in the vertical plane of the line source, $y = 0$, are shown in figure 14 for $Pr = 0.72$. Below the heat source the fluid initiates its motion in a direction perpendicular to the line source, but the flow is gradually deflected towards the direction of gravity.

REFERENCES

COLLIS, D. C. & WILLIAMS, M. J. 1954 Free convection of heat from fine wires. *A.R.L. Aero.* note 140.

DESCHAMPS, V. & DESRAYAUD, G. 1994 Modeling a horizontal heat-flux cylinder as a line source. *J. Thermophys.* **8**, 84–91.

DESRAYAUD, G. & LAURIAT, G. 1993 Unsteady confined boundary plumes. *J. Fluid Mech.* **252**, 617–646.

FAROUK, B. & GÜÇERI, S. I. 1981 Natural convection from a horizontal cylinder – laminar regime. *Trans. ASME* C: *J. Heat Transfer* **103**, 522–527.

FUJII, T. 1963 Theory of the steady laminar convection above a horizontal line heat source and point heat source. *Intl J. Heat Mass Transfer* **6**, 597–606.

FUJII, T., FUJII, M. & MATSUNAGA, T. 1979 A numerical analysis of laminar free convection around an isothermal horizontal circular cylinder. *Numer. Heat Transfer* **2**, 329–344.

FUJII, T., MORIOKA, I. & UEHARA, H. 1973 Buoyant plume above a horizontal line heat source. *Intl J. Heat Mass Transfer* **16**, 755–768.

GEBHART, B., JALURIA, Y., MAHAJAN, R. L. & SAMMAKIA, B. 1988 *Buoyancy-Induced Flows and Transport*. Springer.

Gebhart, B., Pera, L. & Schorr, A. W. 1970 Steady similar natural convection plumes above a horizontal line source. *Intl J. Heat Mass Transfer* **13**, 161–171.

Haaland, S. E. & Sparrow, E. M. 1973 Stability of buoyant boundary layers and plumes, taking account of non-parallelism of the basic flows. *Trans. ASME* C: *J. Heat Transfer* **95**, 295–301.

Hermann, R. 1936 Wärmeübertragung bei freier strömung am waagerechten zylinder in zweiatomigen gasen. *VDI Forschungsheft 379* (see also *NASA Tech. Mem.* 1366, 1954).

Hieber, C. A. & Gebhart, B. 1968 Low Reynolds number heat transfer from a circular cylinder *J. Fluid Mech.* **32**, 21–28.

Hieber, C. A. & Nash, E. J. 1975 Natural convection above a line heat source: higher-order effects and stability. *Intl J. Heat Mass Transfer* **18**, 1473–1479.

Hodnett, P. F. 1969 Low Reynolds number flow of a variable property gas past a heated circular cylinder. *J. Fluid Mech.* **39**, 465–476.

Ingham, D. B. & Pop, I. 1987 Natural convection about a heated horizontal cylinder in a porous medium. *J. Fluid Mech.* **184**, 157–181.

Kaplun, S. & Lagerstrom, P. A. 1957 Asymptotic expansions of Navier-Stokes solutions for small Reynolds numbers. *J. Math. Mech.* **6**, 585–593.

Kropinski, M. C. A., Ward, M. J. & Keller, J. B. 1995 A hybrid asymptotic-numerical method for low Reynolds number flows past a cylindrical body. *SIAM J. Appl. Maths* **55**, 1484–1510.

Kuehn, T. H. & Goldstein, R. J. 1980 Numerical solution to the Navier-Stokes equations for laminar natural convection about a horizontal isothermal circular cylinder. *Intl J. Heat Mass Transfer* **23**, 971–979.

Kuiken, H. K. & Rotem, Z. 1971 Asymptotic solution for plume at very large and small Prandtl numbers. *J. Fluid Mech.* **45**, 585–600.

Lauriat, G. & Desrayaud, G. 1994 Buoyant plane plumes from heated horizontal confined wires and cylinders. *Sādhanā* **19**, 671–703.

Leal, L. G. 1992 *Laminar Flow and Convection Transport Processes.* Butterworth-Heinemann.

Mahony, J. J. 1957 Heat transfer at small Grashof numbers. *Proc. R. Soc. Lond.* A **238**, 412–423.

Mörwald, K., Mitsotakis, K. & Schneider, W. 1986 Higher-order analysis of laminar plumes. *Proc. 8th Intl Heat Transfer Conf., San Francisco*, vol. 3, pp. 1335–1340.

Nakai, S. & Okazaki, T. 1975 Heat transfer from a horizontal circular wire at small Reynolds and Grashof number. *Intl J. Heat Mass Transfer* **18**, 387–396.

Riley, N. 1974 Free convection from a horizontal line source of heat. *Z. Angew. Math. Phys.* **25**, 818–828.

Saitoh, T., Sajik, T. & Maruhara, K. 1993 Bench mark solutions to natural convection heat transfer problem around a horizontal circular cylinder. *Intl J. Heat Mass Transfer* **36**, 1251–1259.

Schuh, H. 1948 Boundary layers of temperature. In *Boundary Layers*, by W. Tollmien. British Ministry of Supply, German Document Center, Reference 3220T.

Spalding, D. B. & Cruddace, R. G. 1961 Theory of the steady laminar buoyant flow above a line heat source in a fluid of large Prandtl number and temperature-dependent viscosity. *Intl J. Heat Mass Transfer* **3**, 55–59.

Tamada, K., Miuri, H. & Miyagi, T. 1985 Low-Reynolds-number flow past a cylindrical body. *J. Fluid Mech.* **132**, 445–455.

Vázquez, P. A., Pérez, A. T. & Castellanos, A. 1996 Thermal and electrohydrodynamic plumes. A comparative study. *Phys. Fluids* **8**, 2091–2096.

Yih, C. S. 1952 Laminar free convection due to a line source of heat. *Trans. Am. Geophys. Union*, **33**, 669–672.

Yih, C.-S. 1969 *Fluid Mechanics*, McGraw-Hill.

Zeldovich, Ya. B. 1937 The asymptotic laws of freely-ascending convective flows. *Eksp. Teor. Fiz.* **7**, 1463–1465 (see also *Selected Works of Yakov Borisovich Zeldovich*, Princeton University Press, 1992).